# Use-Dependent Potentiation of the $Na_v1.6$ Sodium Channel

W. Zhou and A. L. Goldin
Department of Microbiology & Molecular Genetics, University of California, Irvine, California 92697-4025

ABSTRACT $Na_v1.2$ and $Na_v1.6$ are two voltage-gated sodium channel isoforms that are abundant in the adult central nervous system. These channels are expressed in different cells and localized in different neuronal regions, which may reflect functional specialization. To examine this possibility, we compared the properties of $Na_v1.2$ and $Na_v1.6$ in response to a rapid series of repetitive depolarizations. Currents through $Na_v1.6$ coexpressed with $\beta1$ demonstrated use-dependent potentiation during a rapid train of depolarizations. This potentiation was in contrast to the use-dependent decrease in current for $Na_v1.2$ with $\beta1$. The voltage dependence of potentiation correlated with the voltage dependence of activation, and it still occurred when fast inactivation was removed by mutation. Rapid stimulation accelerated a slow phase of activation in the $Na_v1.6$ channel that had fast inactivation removed, resulting in faster channel activation. Although the $Na_v1.2$ channel with fast inactivation removed also demonstrated slightly faster activation, that channel showed very pronounced slow inactivation compared to $Na_v1.6$. These results indicate that potentiation of $Na_v1.6$ sodium currents results from faster channel activation, and that this effect is masked by slow inactivation in $Na_v1.2$. The data suggest that $Na_v1.6$ might be more resistant to inactivation, which might be helpful for high-frequency firing at nodes of Ranvier compared to $Na_v1.2$.

## INTRODUCTION

Voltage-gated sodium channels are the transmembrane proteins responsible for the initial rising phase of the action potential in electrically excitable cells (Catterall, 2000; Goldin, 2001). In mammals, there are nine sodium channel $\alpha$-subunit isoforms named $Na_v1.1$–$Na_v1.9$ (Goldin, 2002; Goldin et al., 2000). Three of these ($Na_v1.1$, $Na_v1.2$, and $Na_v1.6$) are expressed at high levels in the adult central nervous system (CNS). The genes encoding $Na_v1.1$ (*SCN1A*) and $Na_v1.2$ (*SCN2A*) are clustered together on chromosome 2 in both mouse and human, whereas the gene encoding $Na_v1.6$ (*SCN8A*) is located on chromosome 15 in mouse and chromosome 12 in human (Litt et al., 1989; Malo et al., 1991, 1994; Plummer et al., 1998). Although the amino acid sequence of $Na_v1.6$ is >84% identical to the sequences of $Na_v1.1$ and $Na_v1.2$, it is more distant from those two than they are to each other (Goldin et al., 2000).

The three adult CNS isoforms are selectively expressed in different cell types and localized in different neuronal regions, which may indicate that they serve different purposes as determined by their electrophysiological properties. Nodes of Ranvier are the axonal regions without myelin and glial cell wrapping, which are essential for the efficient conduction of action potentials. $Na_v1.6$ is the predominant isoform at the nodes of Ranvier in both sensory and motor neurons of the adult CNS and peripheral nervous system (Caldwell et al., 2000). Studies of developing retinal ganglion cells have shown that $Na_v1.2$ and $\beta2$ are clustered at immature nodes of Ranvier. As myelination proceeds, $Na_v1.6$ replaces $Na_v1.2$ (Boiko et al., 2001; Kaplan et al., 2001). Little $Na_v1.6$ and much more of $Na_v1.2$ are detected on myelin-deficient axons of *shiverer* mice (Boiko et al., 2001). $Na_v1.6$ disappears from the nodes after nerve injury (Novakovic, 1999). These data suggest that $Na_v1.6$ may play a critical role in faithfully transmitting high-frequency action potentials, which could reflect unique electrophysiological properties of $Na_v1.6$ compared to $Na_v1.2$.

In this study, we compared the properties of $Na_v1.6$ and $Na_v1.2$ in response to a rapid series of repetitive depolarizations. Previous studies have shown that currents through $Na_v1.1$ and $Na_v1.2$ with or without the auxiliary $\beta$-subunits decrease in response to high-frequency depolarizations (Pugsley and Goldin, 1998; Spampanato et al., 2001). In contrast, currents through $Na_v1.6$ coexpressed with $\beta1$ increased in response to high-frequency depolarizations. The use-dependent potentiation still occurred when fast inactivation was removed by mutation, suggesting that it resulted from changes in channel activation. Consistent with this interpretation, high-frequency depolarizations accelerated a slow phase of activation in the $Na_v1.6$ channel that had fast inactivation removed. The activation kinetics of $Na_v1.2$ with $\beta1$ were faster than those of $Na_v1.6$, so that it might already be close to the maximal rate. Repetitive depolarizations only slightly accelerated the activation kinetics of $Na_v1.2$ with $\beta1$ and the current decreased due to its faster slow inactivation. These results suggest that $Na_v1.6$ might be specialized to more faithfully propagate high-frequency firing at nodes of Ranvier compared to $Na_v1.2$.

## MATERIALS AND METHODS

### Site-directed mutagenesis

The IFM to QQQ mutation was constructed in the *Mfe*I to *Bst*EII fragment containing the III-IV linker of $Na_v1.6$, which was subcloned into pBSTA.

*Submitted May 12, 2004, and accepted for publication September 22, 2004.*

Address reprint requests to A. L. Goldin, Tel.: 949-824-5334; Fax: 949-824-8504; E-mail: agoldin@uci.edu.



0006-3495/04/12/3862/11 $2.00

doi: 10.1529/biophysj.104.045963

Site-directed mutagenesis was performed using the QuikChange site-directed mutagenesis kit (Stratagene, La Jolla, CA). The mutagenesis primers were:

5′CAACAGAAGAAAAAGTTTGGAGGTCAGGACCAGCAGCAG-ACAGAGGAACAGAAGAAGTACTACAACGCC3′ (sense) and
5′GGCGTTGTAGTACTTCTTCTGTTCCTCTGTCTGCTGCTGGTC-CTGACCTCCAAACTTTTTCTTCTGTTG3′ (antisense)

The mutation was confirmed by sequencing. The *Mfe*I to *Bst*EII fragment was then ligated back into the full-length clone to make $Na_v1.6Q3$. The $Na_v1.2Q3$ mutant was previously described (West et al., 1992).

## Expression of the sodium channels $\alpha$- and $\beta$1-subunits in *Xenopus* oocytes

Stage V oocytes were removed from adult female *Xenopus laevis* frogs and prepared as previously described (Goldin, 1991). Oocytes were incubated in ND-96 media, which consists of 96 mM NaCl, 2 mM KCl, 1.8 mM $CaCl_2$, 1 mM $MgCl_2$, and 5 mM HEPES, pH 7.5, supplemented with 0.1 mg/ml gentamicin, 0.55 mg/ml pyruvate, and 0.5 mM theophylline. Plasmids containing the sodium channel wild-type and mutant $\alpha$-subunit or $\beta$1-subunit cDNA were linearized with *Not*I, and capped full-length transcripts were synthesized in vitro using T7 RNA polymerase (mMESSAGE mMACHINE kit; Ambion., Austin, TX). RNA was dissolved in 1 mM Tris-HCl, pH 7.5, and injected into oocytes. The ratio of $\alpha$- to $\beta$1-subunits was 1:10. Oocytes were incubated in ND96 at 20°C for 1–2 days before recording.

## Electrophysiological recording

Electrophysiological recording used either the two-electrode voltage clamp or the cut-open oocyte voltage clamp. The two-electrode voltage clamp experiments were performed using the oocyte clamp OC-725B (Warner Instruments., Hamden, CT), DigiData 1322A interface (DAGAN, Minneapolis, MN), and pCLAMP software (version 8.1, Axon Instruments, Burlingame, CA). The recording solution was ND-96 without supplements. Tetrodotoxin (TTX) subtraction was used to eliminate all non-TTX sensitive currents by subtracting those currents recorded in the presence of 400 nM TTX from those recorded in the absence of TTX.

The cut-open oocyte voltage-clamp experiments were performed using the CA-1 high-performance oocyte clamp (DAGAN), DigiData 1321A interface, and pClamp software (Smith and Goldin, 1998). All recordings were obtained after stable baseline and ionic current levels were achieved. The experiments were performed with an external solution containing (in mM) 120 NaOH-methyl sulfonate, 1.8 $Ca(OH)_2$-methyl sulfonate, and 10 HEPES, pH 7.5. The internal solution consisted of 44 $K_2SO_4$, 5 $Na_2SO_4$, 10 EGTA-Cs, and 10 HEPES-Cs, pH 7.5.

## Data analysis

Data analysis was performed using pCLAMP software (version 8.1, Axon Instruments, Burlingame, CA). Peak conductance was calculated using the following equation:

$$G = I/(V - E_r),$$

in which $G$ is conductance, $I$ is peak inward current, $V$ is the test potential, and $E_r$ is the reversal potential. Reversal potentials were individually estimated for each data set by fitting the I-V data with the equation:

$$I = [1 + \exp(-0.03937 \times z \times (V - V_{1/2}))]^{-1} \times g \times (V - V_r),$$

in which $z$ is the apparent gating charge, $g$ is a factor related to the number of channels contributing to the macroscopic current, $V$ is equal to the voltage potential of the pulse, and $V_{1/2}$ is the half-maximal voltage. The normalized conductance was fit to a two-state Boltzmann function of the form:

$$G/G_{max} = 1/(1 + \exp((-0.3937 \times z \times (V - V_{1/2}))),$$

in which $z$, $V$, and $V_{1/2}$ have the same meaning.

The kinetics of fast inactivation were analyzed by fitting the current traces between 0.4 ms after the peak current and the end of the 20-ms depolarization with a double exponential equation:

$$I = A_s \times \exp(-t/\tau_s) + A_f \times \exp(-t/\tau_f) + C,$$

in which $I$ is the current amplitude, $\tau_s$ is the slow time constant of inactivation, $\tau_f$ is the fast time constant of inactivation, $A_s$ and $A_f$ are the percentages of current inactivating with the slow and fast time constants, respectively, and $C$ is the noninactivating current.

The kinetics of activation were analyzed by fitting the current traces between the start of activation and the peak current with either a single or double exponential equation of the form:

$$I = A_s \times (1 - \exp(-(t-k)/\tau_s)) + A_f \times (1 - \exp(-(t-k)/\tau_f)),$$

in which $I$ is the current amplitude, $k$ is the time shift, $\tau_s$ is the slow time constant of activation, $\tau_f$ is the fast time constant of activation, and $A_s$ and $A_f$ are the percentages of current activating with the slow and fast time constants, respectively. The choice of a single exponential equation for $Na_v1.2$ and a double exponential equation for $Na_v1.6$ was made empirically by fitting activation for both channels with both types of equations and visually inspecting the quality of the fits.

The kinetics of slow inactivation were analyzed by fitting the current traces between the peak current and the end of the 10-s depolarization with a double exponential equation:

$$I = A_s \times \exp(-t/\tau_s) + A_f \times \exp(-t/\tau_f),$$

in which $I$ is the current amplitude, $\tau_s$ is the slow time constant of inactivation, $\tau_f$ is the fast time constant of inactivation, and $A_s$ and $A_f$ are the percentages of current inactivating with the slow and fast time constants, respectively.

# RESULTS

## Currents through $Na_v1.6$ with $\beta$1 increase with rapid stimulation

There are nine sodium channel isoforms in mammals, three of which are widely expressed in the adult CNS ($Na_v1.1$, $Na_v1.2$, and $Na_v1.6$) (Goldin, 2001). Two of these isoforms ($Na_v1.1$ and $Na_v1.2$) demonstrate a decrease in current with repetitive depolarizations (Pugsley and Goldin, 1998; Spampanato et al., 2001), which might limit their ability to propagate high-frequency action potentials. Because $Na_v1.6$ is the primary channel at nodes of Ranvier (Caldwell et al., 2000), that channel might have different characteristics that enable it to sustain high-frequency firing in myelinated axons. To test this possibility, we examined the current through $Na_v1.6$ compared to $Na_v1.2$ during a 10-Hz train of 20 depolarizations, each 20-ms long from −100 mV to −10 mV. The peak current during each depolarization was normalized to the peak current during the first depolarization and plotted against the depolarization number (Fig. 1, *A* and *B*). The first and the last traces of the 20 depolarizations are shown in Fig. 1, *C–F*. When the $\alpha$-subunit of $Na_v1.6$ or

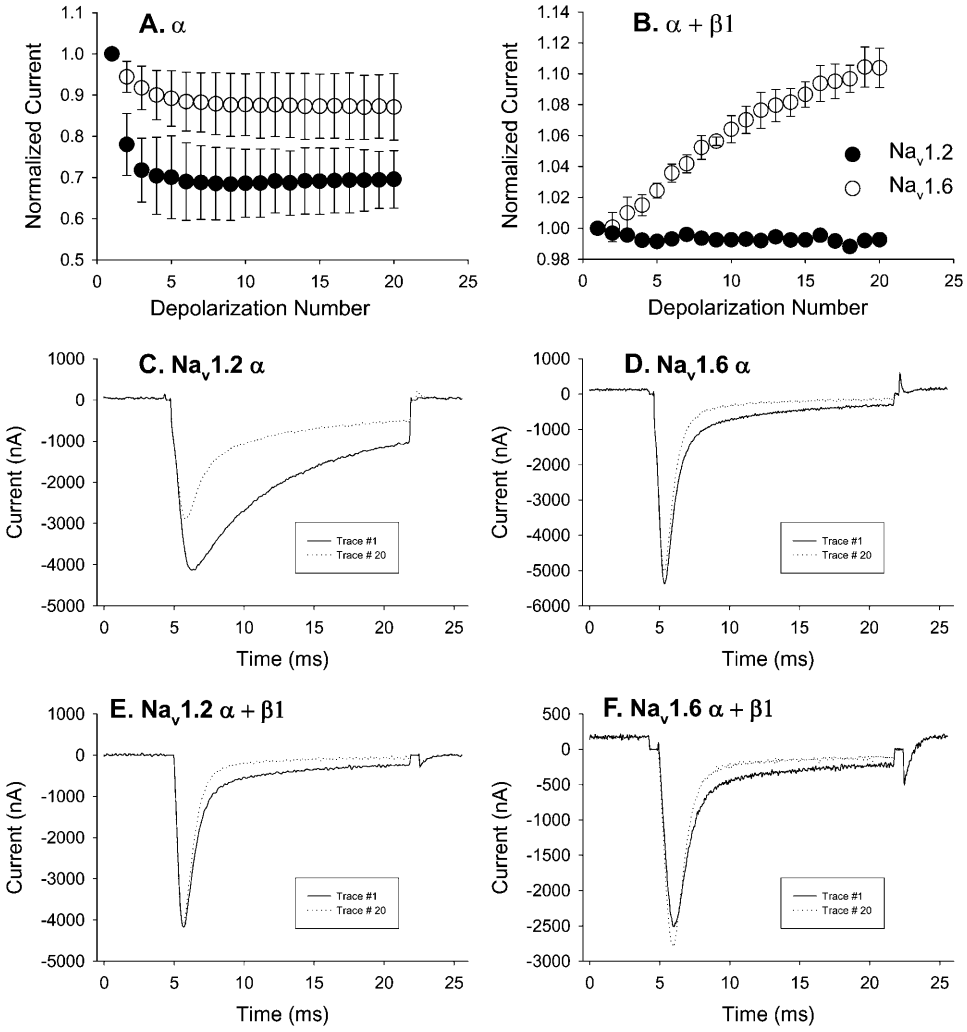


FIGURE 1 (*A*) Average normalized peak currents for $Na_v1.2$ (●; $n = 3$) and $Na_v1.6$ (○; $n = 8$) $\alpha$-subunit sodium channels during repetitive stimulation. (*B*) Average normalized peak currents for $Na_v1.2$ (●; $n = 4$) and $Na_v1.6$ (○; $n = 5$) $\alpha + \beta1$ subunit sodium channels during repetitive stimulation. Currents were recorded in ND96 using a two-electrode voltage clamp with TTX subtraction. The recording protocol consisted of 20 depolarizations of 20-ms duration from −100 mV to −10 mV at 100-ms intervals. The peak current during each depolarization was normalized to the peak current during the first depolarization and plotted against the depolarization number. The symbols represent the means and the error bars indicate the standard deviations. Current traces during the first (*solid line*) and last (*dotted line*) depolarization are shown for $Na_v1.2$ $\alpha$ (*C*), $Na_v1.6$ $\alpha$ (*D*), $Na_v1.2$ $\alpha + \beta1$ (*E*), and $Na_v1.6$ $\alpha + \beta1$ (*F*) sodium channels.

$Na_v1.2$ was expressed alone, the current decreased and reached a steady-state level (panels *A*, *C*, and *D*). The use-dependent decrease in current for $Na_v1.6$ was less pronounced than that for $Na_v1.2$. In contrast, when $Na_v1.6$ was coexpressed with the $\beta1$-subunit, the channel demonstrated an increase in current with successive depolarizations (panels *B* and *F*). $Na_v1.2$ with $\beta1$ demonstrated no significant change in current amplitude under the same set of conditions (panels *B* and *E*).

To analyze the use-dependent potentiation of $Na_v1.6$ with $\beta1$, we designed a protocol to monitor the time course during and after repetitive stimulation (Fig. 2 *A*). First, three 20-ms depolarizations from −120 mV to −10 mV at 1-min intervals were applied to determine the basal level of current. This was followed by rapid stimulation consisting of 200 depolarizations to −10 mV at 100-ms intervals (10 Hz). We used 200 depolarizations because the current through $Na_v1.6$ with $\beta1$ was still increasing at the end of 20 depolarizations, even though the current decrease with $Na_v1.2$ had stabilized after five depolarizations (Fig. 1, *A* and *B*). This was followed by a recovery period consisting of 15 depolarizations to −10 mV at 10-s intervals to determine if potentiation could be reversed at hyperpolarized potentials, similar to the recovery from the use-dependent decrease in current for $Na_v1.2$. Finally, three depolarizations to −10 mV at 1-min intervals were applied to determine if the current had stabilized. To compare the data, the current during each depolarization was normalized to the current during the first depolarization of the entire protocol.

Fig. 2 *B* shows the normalized peak current through $Na_v1.2$ $\alpha$ with $\beta1$ during this protocol. The current level was stable during the baseline depolarizations at 1-min intervals (*open circles*), suggesting that 1 min provides sufficient time for all of the channels to return to the original state. The current decreased during the period of rapid stimulation (*open squares*), consistent with previous results for $Na_v1.2$ (Pugsley and Goldin, 1998). The current returned to the original level after only three depolarizations at 10-s intervals (*open triangles*). The fact that complete recovery required >10 s was surprising because complete recovery was

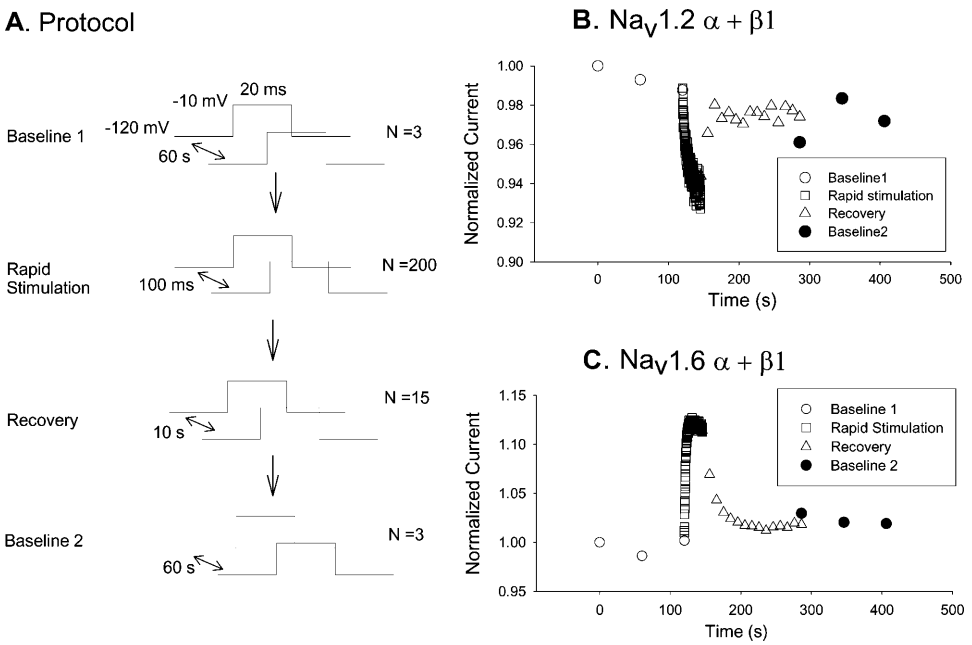


FIGURE 2 (*A*) The recording protocol used to monitor the effects of rapid stimulation. Three 20-ms depolarizations from −120 mV to −10 mV at 1-min intervals were applied to determine the basal level of current. This was followed by rapid stimulation consisting of 200 depolarizations to −10 mV at 100-ms intervals. The stimulation was followed by a recovery protocol consisting of 15 depolarizations to −10 mV at 10-s intervals. Finally, three depolarizations to −10 mV at 1-min intervals were applied to determine the basal level of current at the end of the experiment. (*B*) The normalized peak current in an oocyte expressing $Na_v1.2$ $\alpha$ + $\beta1$ during one application of the protocol shown in panel *A*. The peak current during each depolarization was normalized to the peak current during the first depolarization of the entire protocol and plotted against time. (*B*) The normalized peak current in an oocyte expressing $Na_v1.6$ $\alpha + \beta1$ during one application of the protocol.

obtained within 300 ms when current through $Na_v1.2$ with $\beta1$ was fully inactivated with a single 50-ms depolarization (Smith et al., 1998). This difference could be due to the fact that the total depolarization time in this experiment was 4 s (200 depolarizations of 20 ms each), which would have caused some of the channels to enter the slow inactivated state. Depolarization to −10 mV for 4 s results in slow inactivation of ~80% of current through $Na_v1.1$ with $\beta1$, and it takes significantly longer to recover from slow inactivation than from fast inactivation (Spampanato et al., 2001).

In contrast to the results with $Na_v1.2$, current through $Na_v1.6$ with $\beta1$ increased with successive depolarizations and didn't stabilize until after ~50 depolarizations (Fig. 2 *C*, *open squares*). The current gradually returned to the baseline level during the recovery period (*open triangles*), although it required seven depolarizations (60 s) for complete recovery. This recovery time was approximately three times as long as the time required for $Na_v1.2$ with $\beta1$ to recover from the current decrease, suggesting that the two changes are not the result of comparable processes. The current remained steady during the 1-min intervals at the end of the protocol (*solid circles*), demonstrating that the potentiation was due to the high-frequency depolarizations.

To examine the effect of rapid stimulation on the kinetics of fast inactivation, the current traces during the first (*solid line*) and last (*dotted line*) depolarizations of rapid stimulation were plotted together for $Na_v1.2$ with $\beta1$ (Fig. 3 *A*) and $Na_v1.6$ with $\beta1$ (Fig. 3 *B*). Rapid stimulation accelerated the fast inactivation of both $Na_v1.2$ and $Na_v1.6$. The current traces were fit with a double exponential equation to quantitatively compare the kinetics of fast inactivation, and the results are shown in Table 1. For $Na_v1.2$, rapid stimulation accelerated all aspects of fast inactivation, whereas for $Na_v1.6$ the primary effects were a large increase in the percentage of current inactivating with the fast time constant and a decrease in the amount of persistent current.

Rapid stimulation also appeared to affect the activation kinetics of $Na_v1.6$. The rate of rise for $Na_v1.6$ current is slightly faster and the time to peak is slightly sooner for the trace during the final depolarization (Fig. 3 *B*, *dotted line*) compared to that during the initial depolarization (*solid line*). In contrast, there was no detectable change in the activation kinetics of $Na_v1.2$ after rapid stimulation (Fig. 3 *A*). It is difficult to accurately measure the kinetics of activation in these experiments because of the overlap with fast inactivation, but a quantitative analysis using mutant channels with fast inactivation removed will be presented later.

## $Na_v1.6$ potentiation depends on the extent of activation and inactivation

To examine the relationship between the use-dependent potentiation of $Na_v1.6$ and channel activation, we compared the voltage dependence of both processes. The voltage dependence of activation for the $Na_v1.6$ $\alpha$-subunit alone (Fig. 4 *A*, *open squares*) was 3.7 mV more positive than that for the $Na_v1.2$ $\alpha$-subunit alone (Fig. 4 *A*, *open circles*; Table 2). Coexpression of the $\beta1$-subunit shifted the voltage dependence of activation for both channels to more negative values that were similar (Fig. 4 *B*; Table 2). To determine the voltage dependence of potentiation for $Na_v1.6$ with $\beta1$, the current increase during a series of depolarizations to different voltages was measured by comparing the current amplitude during the first depolarization of the recovery interval with

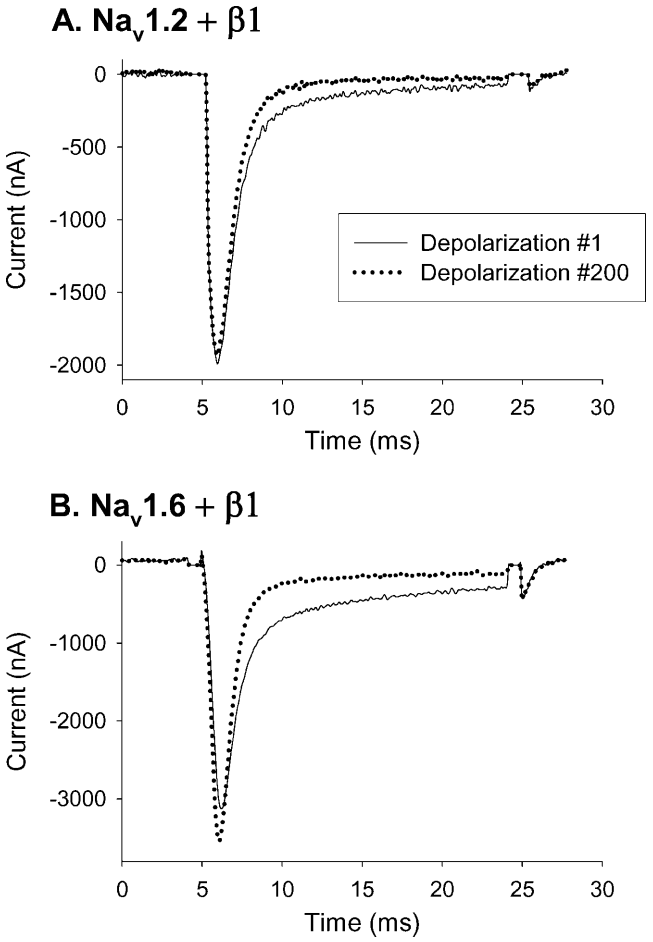


FIGURE 3 Effects of rapid stimulation on the kinetics of sodium channel inactivation. Current traces from oocytes expressing $Na_v1.2$ $\alpha + \beta1$ (*A*) or $Na_v1.6$ $\alpha + \beta1$ (*B*) are shown for the first (*solid line*) and last (*dotted line*) depolarization during the rapid-stimulation protocol shown in Fig. 2 *A*.

that of the last depolarization of the baseline interval. The increase was compared to the current change observed during repetitive depolarizations to −50 mV, at which potential there was no potentiation with rapid stimulation. The amount of increase was normalized to the maximal increase in current, and the data from different oocytes were averaged and plotted against the depolarization voltage (Fig. 4 *C*). The potentiation increased from −40 mV to 0 mV, at which voltage the increase stabilized. The relationship is similar to that observed for the voltage dependence of activation, with a $V_{1/2}$ of ~−17 mV. These results suggest that the increased current of $Na_v1.6$ with $\beta1$ correlates with the extent of channel activation during rapid stimulation.

**TABLE 1 Kinetics of fast inactivation during repetitive stimulation**

| Channel | $Na_v1.2 + \beta1$ ($n = 4$) | | $Na_v1.6 + \beta1$ ($n = 5$) | |
|---|---|---|---|---|
| Depolarization # | 1 | 200 | 1 | 200 |
| Inactivation $\tau_{fast}$ (ms) | 0.94 ± 0.11 | 0.81 ± 0.12 | 0.81 ± 0.08 | 0.71 ± 0.03 |
| Inactivation $\tau_{slow}$ (ms) | 6.73 ± 0.84 | 4.13 ± 0.03 | 4.89 ± 0.12 | 5.73 ± 0.30 |
| Percentage of $\tau_{fast}$ (%) | 68 ± 9 | 82 ± 6 | 58 ± 9 | 88 ± 2 |
| Persistence (%) | 4 ± 1 | 1 ± 1 | 19 ± 3 | 3 ± 1 |

The current increase of $Na_v1.6$ with $\beta1$ was similar to the current decrease of $Na_v1.2$ with $\beta1$ in that they both occurred with rapid stimulation and they both recovered during hyperpolarization. The potentiation of $Na_v1.6$ with $\beta1$ occurred despite the fact that the channels should be inactivating, because the 20-ms depolarization is long enough to fully fast inactivate the channels. However, the 100-ms repolarization time between depolarizations is long enough to allow recovery of most fast inactivated channels. With longer depolarization times, channels might be shifted into the slow inactivated state. To examine the relationship between slow inactivation and the potentiation of $Na_v1.6$ with $\beta1$, we varied the extent of slow inactivation by changing the depolarization time from 10 to 80 ms. Although a single depolarization of 80 ms is too short to result in significant slow inactivation, the cumulative effect of multiple short depolarizations can act like a single long depolarization and result in slow inactivation. The current increase for each depolarization time was compared to the change in current for a 160-ms depolarization time, which showed no significant potentiation and thus served as an internal control. The amount of increase was normalized to the maximal increase in current, and the data from different oocytes were averaged and plotted against the depolarization time (Fig. 5 *A*).

The increase in $Na_v1.6$ current became larger with longer depolarization times from 10 to 30 ms. After 30 ms, longer depolarization times resulted in smaller increases. The fact that the increase became larger for depolarization times up to 30 ms could indicate that the maximal increase required complete activation of the channels during rapid stimulation, which did not occur until 30 ms. Although the current amplitude reached a peak in <5 ms, the peak current may not reflect complete activation because channels begin to fast inactivate before activation is complete. The smaller increase for times longer than 30 ms could result from slow inactivation, which becomes prominent at longer depolarization times.

Because rapid stimulation with depolarization times shorter than 30 ms resulted in smaller increases in current, it is possible that very short depolarizations that would be more similar to those during an action potential might not result in any potentiation. To test this possibility, a rapid-stimulation protocol was performed using 2-ms depolarizations from −120 to −10 mV. The normalized current amplitude during each depolarization was plotted against the depolarization number for $Na_v1.2$ or $Na_v1.6$ with $\beta1$ (Fig. 5 *B*). With 2-ms depolarizations, current through $Na_v1.6$ with $\beta1$ still increased slightly in response to rapid stimulation, whereas current through $Na_v1.2$ with $\beta1$ decreased very slightly.

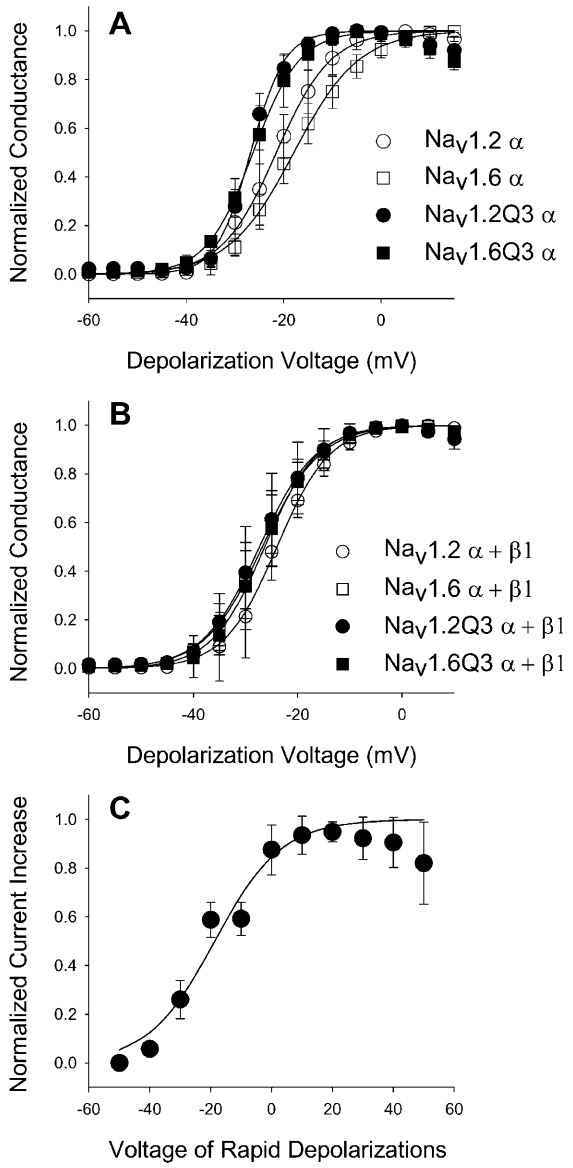


FIGURE 4 (*A*) Voltage dependence of activation for $Na_v1.2$ (○; $n = 4$), $Na_v1.6$ (□; $n = 5$), $Na_v1.2Q3$ (●; $n = 4$), and $Na_v1.6Q3$ (■; $n = 3$) $\alpha$-subunits alone. (*B*) Voltage dependence of activation for $Na_v1.2$ (○; $n = 5$), $Na_v1.6$ (□; $n = 3$), $Na_v1.2Q3$ (●; $n = 4$), and $Na_v1.6Q3$ (■; $n = 4$) $\alpha + \beta1$ subunits. (*C*) Average normalized current increase with different depolarization voltages during rapid stimulation. The current increase during a series of depolarizations to different voltages was compared to the current increase observed during repetitive depolarizations to −50 mV, at which potential there was no potentiation with rapid stimulation. The amount of increase was normalized to the maximal increase in current, and the data from different oocytes were averaged and plotted against the depolarization voltage ($n = 6$). Although the rapid-stimulation depolarizations were to a range of different voltages, the depolarizations during the baseline1, recovery and baseline2 intervals were all to −10 mV, and potentiation was determined from depolarizations to −10 mV by comparing the first depolarization of the recovery interval to the last depolarization of the baseline1 interval. Recordings were obtained using the two-electrode voltage clamp with TTX subtraction for all data except the voltage dependence of activation of $Na_v1.2$ and $Na_v1.6$ with and without $\beta1$, for which the cut-open oocyte voltage clamp was used. The symbols represent the means and the error bars indicate the standard deviations.

**TABLE 2 Parameters of voltage-dependent activation**

| | $\alpha$ | | | $\alpha + \beta1$ | | |
|---|---|---|---|---|---|---|
| Channel | $V_{1/2}$ (mV) | $z$ ($e_0$) | $n$ | $V_{1/2}$ (mV) | $z$ ($e_0$) | $n$ |
| $Na_v1.2$ | −21.6 ± 2.4 | 5.0 ± 1.5 | 3 | −24.3 ± 2.7 | 5.5 ± 1.4 | 4 |
| $Na_v1.6$ | −17.9 ± 2.3 | 3.9 ± 3.0 | 5 | −26.8 ± 2.7 | 4.8 ± 0.5 | 4 |
| $Na_v1.2Q3$ | −27.2 ± 1.5 | 7.6 ± 1.3 | 5 | −27.2 ± 4.2 | 5.3 ± 0.6 | 4 |
| $Na_v1.6Q3$ | −27.6 ± 3.2 | 5.1 ± 0.6 | 5 | −25.9 ± 3.5 | 5.5 ± 0.6 | 4 |

## Potentiation of $Na_v1.6$ is unstable at hyperpolarized potentials

The return of current to the baseline level after repetitive depolarizations suggests that the increase was unstable at negative potentials. To examine the stability of the current increase, we varied the time between depolarizations from 100 to 1000 ms. The current increase for each time interval between depolarizations was compared to the change in current with a 2-s interval, for which time there was no significant potentiation. The amount of increase was normalized to the maximal increase in current, and the data from different oocytes were averaged and plotted against the time interval (Fig. 5 *C*). The increase was larger with smaller time intervals, corresponding to a higher frequency of depolarization. This result demonstrates that the channels recover from the current increase during the intervals of hyperpolarization between depolarizations during rapid stimulation, similar to the recovery from inactivation at negative potentials.

## Potentiation of $Na_v1.6$ results from faster activation

The data thus far suggest that the increase of $Na_v1.6$ with $\beta1$ during rapid stimulation might be caused by increasing channel activation. To examine the kinetics of activation, we removed fast inactivation from both $Na_v1.2$ and $Na_v1.6$ by replacing the critical isoleucine, phenylalanine, and methionine (IFM) residues in the III-IV linker inactivation particles with three glutamine residues (West et al., 1992). The noninactivating channels were termed $Na_v1.2Q3$ and $Na_v1.6Q3$. Activation was elicited from a holding potential of −120 mV by 200-ms depolarizations to potentials ranging between −80 and 50 mV (Fig. 6). Sample traces from oocytes expressing $Na_v1.2$ and $Na_v1.2Q3$ $\alpha$-subunits are shown in Fig. 6, *A* and *B*. The currents through $Na_v1.2$ were fully inactivated within 100 ms, whereas there was no significant inactivation of $Na_v1.2Q3$ current during the 200-ms depolarization. Similarly, currents through $Na_v1.6$ were fully inactivated within 100 ms and there was no significant inactivation of $Na_v1.6Q3$ current during the 200-ms depolarization (Fig. 6, *C* and *D*). $Na_v1.2Q3$ and $Na_v1.6Q3$ demonstrated similar voltage dependences of activation that were more negative than those for $Na_v1.2$ and $Na_v1.6$ (Fig. 4 *A* and Table 2). Coexpression of $\beta1$ did not affect the voltage

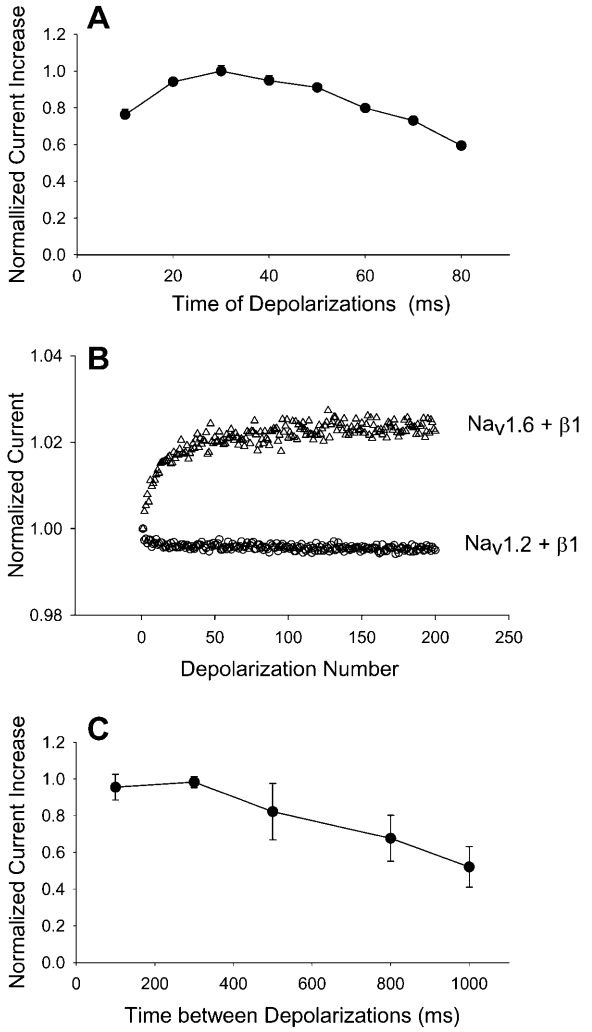


FIGURE 5 (*A*) Average normalized current increase with different depolarization times during rapid stimulation. The current increase for different times of depolarization to −10 mV was compared to the change in current for 160 ms, because there was no significant potentiation in current when the depolarization time was 160 ms. The time between depolarizations was constant. The amount of increase was normalized to the maximal increase in current, and the data from different oocytes were averaged and plotted against the depolarization time ($n = 4$). The symbols represent the means and the error bars indicate the standard deviations. (*B*) The peak current amplitudes through $Na_v1.2$ with $\beta1$ (○) and $Na_v1.6$ with $\beta1$ (△) during 200 depolarizations from −100 to −10 mV, each lasting 2 ms. The current amplitudes were normalized to the peak current amplitude during the initial depolarization. The data were recorded using the cut-open oocyte voltage clamp as described in Materials and Methods. (*C*) Average normalized current increase levels with different time intervals between depolarizations during rapid stimulation. The current increase for different time intervals between depolarization was compared to the change in current with a 2-s interval, because there was no significant potentiation in current with a 2-s interval. The amount of increase was normalized to the maximal increase in current, and the data from different oocytes were averaged and plotted against the time interval ($n = 5$). Recordings were obtained in ND96 using a two-electrode voltage clamp. The symbols represent the means and the error bars indicate the standard deviations.

dependence of activation for $Na_v1.2Q3$ nor that of $Na_v1.6Q3$, whereas the voltage dependences of activation for $Na_v1.2$ and $Na_v1.6$ were both shifted toward the values of the noninactivating mutants in the presence of $\beta1$ (Fig. 4 *B* and Table 2). These data suggest that both the differences in the voltage dependence of activation between wild-type $Na_v1.2$ and $Na_v1.6$ and the effects of the $\beta1$-subunit on the voltage dependence of activation are due to fast inactivation.

We then compared the activation kinetics of the noninactivating channels. The current traces during depolarizations from −120 mV to −10 mV were normalized to the peak current and plotted together (Fig. 6, *E* and *F*). The $Na_v1.2Q3$ $\alpha$-subunit channel (Fig. 6 *E*, *dotted line*) activated significantly faster than the $Na_v1.6Q3$ $\alpha$-subunit channel (*solid line*). Coexpression of the $\beta1$-subunit speeded up the activation of both channels so that activation appeared equivalent on this timescale (Fig. 6 *F*). There was no significant inactivation of $Na_v1.6Q3$ with $\beta1$ (Fig. 6 *F*, *solid line*), but the $Na_v1.2Q3$ with $\beta1$ channel showed a decrease in current of ~20% by the end of the 200-ms depolarization (*dotted line*), presumably due to slow inactivation. These data suggest that $Na_v1.2$ enters the slow inactivated state more rapidly than $Na_v1.6$.

The responses of the noninactivating channels to rapid stimulation were examined using the protocol shown in Fig. 2 *A*. $Na_v1.2Q3$ with $\beta1$ showed a slight increase in current during the first 10 depolarizations of rapid stimulation, after which the current decreased with successive depolarizations (Fig. 7 *A*, *open squares*). Currents through $Na_v1.6Q3$ with $\beta1$ also showed an increase during repetitive stimulation, but in this case the increase was larger and it continued for 30 depolarizations (Fig. 7 *B*). The increase was followed by a decrease in current, similar to the results with $Na_v1.2Q3$. The decrease in current for both $Na_v1.2Q3$ and $Na_v1.6Q3$ with $\beta1$ did not appear to stabilize, in contrast to the decrease for $Na_v1.2$ with $\beta1$ (Fig. 2 *B*). Because fast inactivation had been eliminated in $Na_v1.2Q3$ and $Na_v1.6Q3$, the continuing decrease in current was most likely due to accumulation of slow inactivation.

To determine if repetitive stimulation altered the kinetics of activation for $Na_v1.2Q3$ or $Na_v1.6Q3$ with $\beta1$, the current traces during the first depolarization, the depolarization during which potentiation was maximal (10 for $Na_v1.2Q3$ and 30 for $Na_v1.6Q3$), and the last depolarization were plotted together (Fig. 7, *C* and *D*). For $Na_v1.2Q3$, activation was slightly faster during the tenth depolarization (*dotted line*) compared to the first depolarization (*solid line*), and it remained faster during the final depolarization (*dashed line*). Similarly, activation of $Na_v1.6Q3$ was faster during the thirtieth depolarization (*dotted line*) compared to the first depolarization (*solid line*), and it remained faster during the final depolarization (*dashed line*). To quantify these effects, the current traces were fit using a double exponential equation for $Na_v1.6Q3$ and a single exponential equation for $Na_v1.2Q3$, because there was only one component of

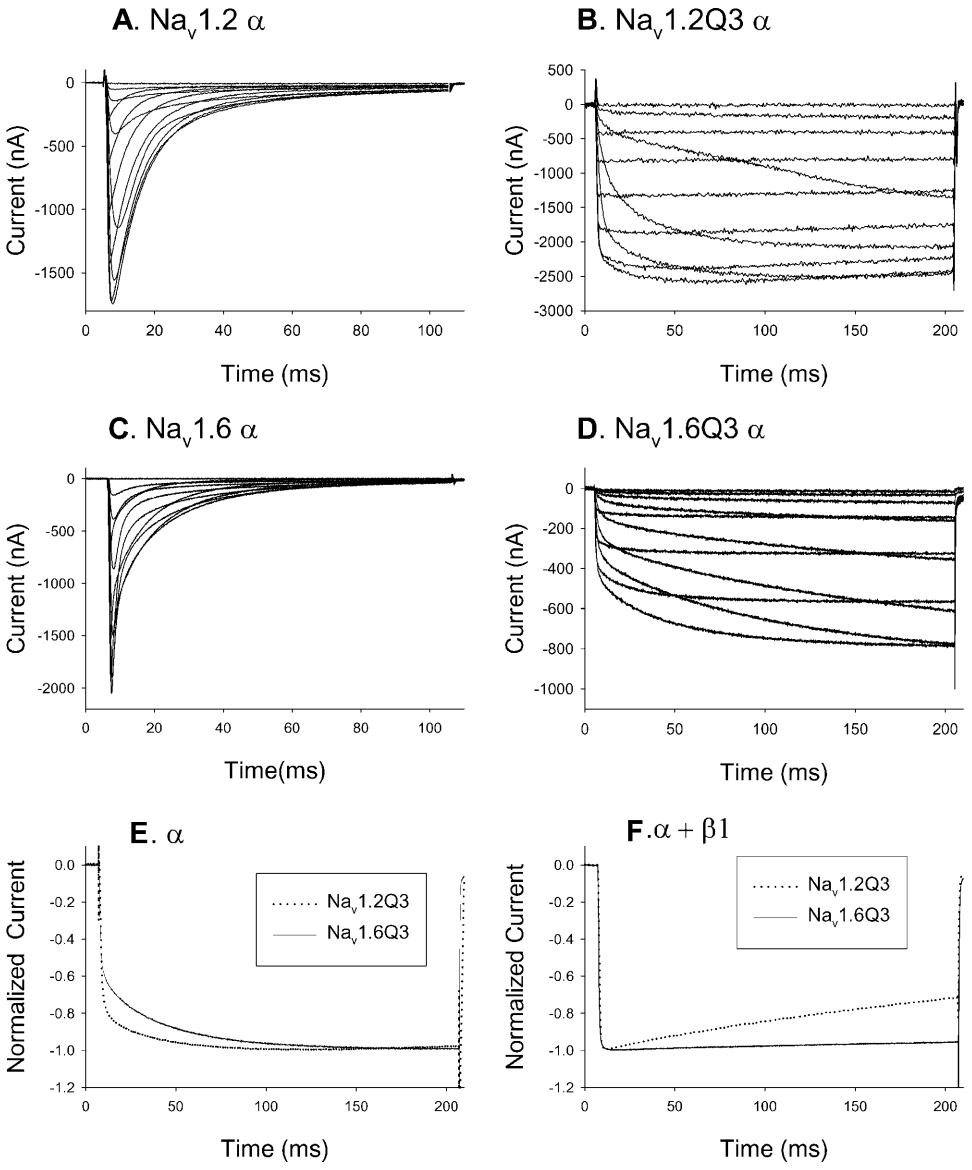


FIGURE 6 (*A*) Current traces from an oocyte expressing $Na_v1.2$ $\alpha$-subunit sodium channels. The oocyte was depolarized from −120 mV to potentials ranging from −90 to 50 mV. The traces shown are for depolarizations to −50 mV, between −35 and 25 mV in 10-mV increments and to 35 mV. (*B*) Current traces from an oocyte expressing $Na_v1.2Q3$ $\alpha$-subunit sodium channels. The traces shown are for depolarizations to −45 mV, between −35 and 25 mV in 10-mV increments and to 35 mV. (*C*) Current traces from an oocyte expressing $Na_v1.6$ $\alpha$-subunit sodium channels. The traces shown are for depolarizations to −50 mV, between −35 and 25 mV in 10-mV increments and to 35 mV. (*D*) Current traces from an oocyte expressing $Na_v1.6Q3$ $\alpha$-subunit sodium channels. The traces shown are for depolarizations to −45 mV, between −35 and 25 mV in 10-mV increments and to 35 mV. (*E*) Normalized current traces for $Na_v1.2Q3$ (*dotted line*) and $Na_v1.6Q3$ (*solid line*) $\alpha$-subunits during depolarizations from −120 mV to −10 mV for 200 ms. (*F*) Normalized current traces for $Na_v1.2Q3$ (*dotted line*) and $Na_v1.6Q3$ (*solid line*) $\alpha + \beta1$ subunits during depolarizations from −120 mV to −10 mV for 200 ms. The data were recorded using the cut-open oocyte voltage clamp as described in Materials and Methods.

activation for that channel as determined by fitting activation for each channel with both types of equations. The time constant for $Na_v1.2Q3$ activation was slightly faster by the tenth depolarization, and it remained at the same level during the final depolarization (Table 3). For $Na_v1.6Q3$, both the fast and slow time constants were faster and the percentage of current activating with the fast time constant was larger by the thirtieth depolarization, and all three values stayed at similar levels during the final depolarization (Table 3). These results suggest that the larger increase in current through $Na_v1.6Q3$ compared to $Na_v1.2Q3$ might be partially due to the more pronounced acceleration of activation for $Na_v1.6Q3$ compared to $Na_v1.2Q3$.

A second factor that could account for the larger increase in current through $Na_v1.6Q3$ compared to $Na_v1.2Q3$ is slow inactivation, which occurred more rapidly for $Na_v1.2Q3$ (Fig. 6 *F*). To examine the kinetics of slow inactivation, oocytes expressing $Na_v1.2Q3$ or $Na_v1.6Q3$ both with and without $\beta1$ were depolarized from −120 mV to −10 mV for 10 s. Currents were normalized to the peak current amplitude and plotted together (Fig. 8). The current traces were fit with a double exponential equation, and the time constants are shown in Table 4. Slow inactivation of $Na_v1.2Q3$ was significantly faster than that of $Na_v1.6Q3$. Although both of the time constants for $Na_v1.6Q3$ were smaller than those for $Na_v1.2Q3$, the major difference was that 58% of $Na_v1.2Q3$ current slow inactivated with the fast time constant whereas only 6% of $Na_v1.6Q3$ current slow inactivated with the fast time constant. Coexpression of $\beta1$ accelerated the slow inactivation of $Na_v1.2Q3$ considerably by decreasing both the fast and slow time constants. In contrast, $\beta1$ slowed the slow inactivation of $Na_v1.6Q3$ by increasing the slow time constant, despite a small decrease in the fast time constant. These data suggest that the faster entry of $Na_v1.2Q3$

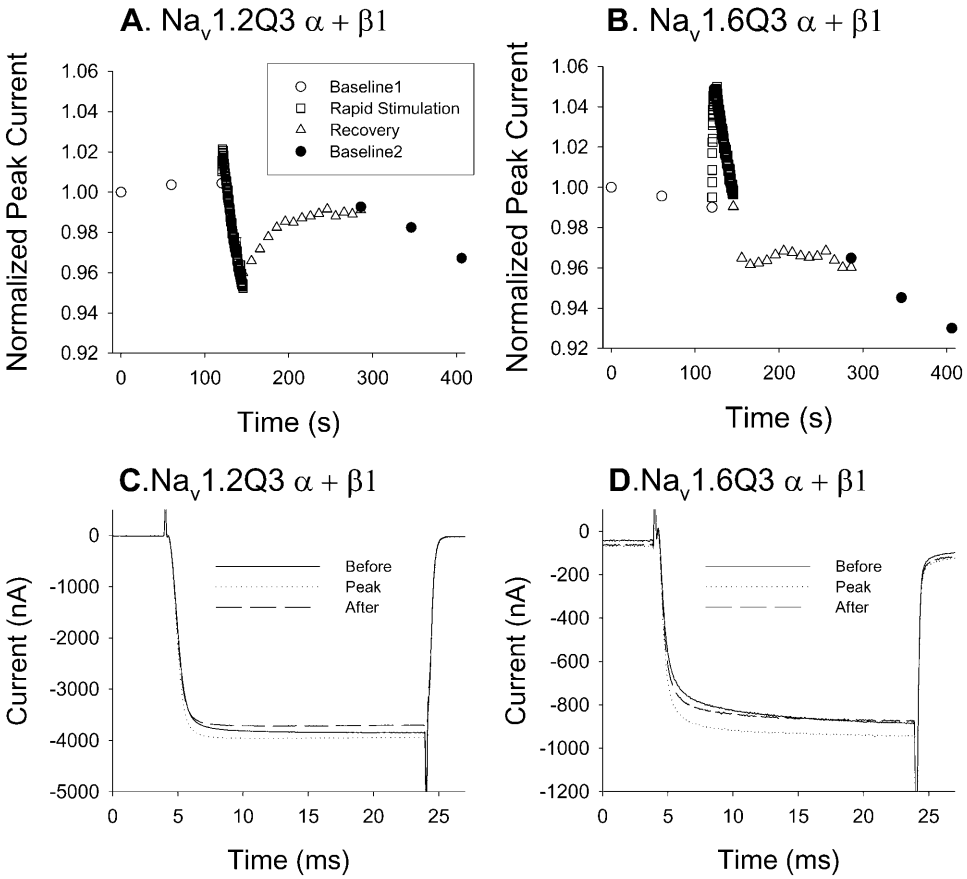


FIGURE 7 (*A*) The normalized peak currents from an oocyte expressing $Na_v1.2Q3$ $\alpha + \beta1$ during one application of the rapid-stimulation protocol shown in Fig. 2 *A*. (*B*) The normalized peak currents from an oocyte expressing $Na_v1.6Q3$ $\alpha + \beta1$ during one application of the rapid-stimulation protocol shown in Fig. 2 *A*. (*C*) The first (*solid line*), tenth (*dotted line*), and last (*dashed line*) current trace for $Na_v1.2Q3$ $\alpha + \beta1$ during the rapid-stimulation protocol. (*D*) The first (*solid line*), thirtieth (*dotted line*), and last (*dashed line*) current trace for $Na_v1.6Q3$ $\alpha + \beta1$ during the rapid-stimulation protocol. The data were recorded using the cut-open oocyte voltage clamp as described in Materials and Methods.

channels into the slow inactivated state resulted in the transient potentiation of $Na_v1.2Q3$ during rapid stimulation compared to $Na_v1.6Q3$ (Fig. 7, *A* and *B*).

## DISCUSSION

In this study, we have shown that sodium channels consisting of $Na_v1.6$ plus the $\beta1$-subunit demonstrate use-dependent potentiation during a rapid train of depolarizations. This potentiation is in contrast to the use-dependent decrease in current for the other adult mammalian CNS sodium channels ($Na_v1.1$ and $Na_v1.2$) during a comparable train of depolarizations (Pugsley and Goldin, 1998; Spampanato et al., 2001). The extent of $Na_v1.6$ potentiation increased with increasing depolarization times up to 30 ms, and it decreased with increasing times between depolarizations. The voltage dependence of potentiation correlated with the voltage dependence of activation, and the kinetics of activation were accelerated after rapid stimulation.

One mechanism to explain the potentiation of $Na_v1.6$ with $\beta1$ is that repetitive depolarizations cause faster channel activation. Four characteristics of the use-dependent potentiation are consistent with this hypothesis. First, the voltage dependence of potentiation correlated with the voltage dependence of activation (Fig. 4). Second, potentiation occurred with sodium channels in which fast inactivation had been removed (Fig. 7 *B*). Third, the potentiation of $Na_v1.6$ with $\beta1$ increased with increasing depolarization times up to 30 ms (Fig. 4 *A*), and activation of $Na_v1.6Q3$ with $\beta1$ continued to increase until at least 20 ms (Fig. 7 *D*). Finally, the kinetics of activation for $Na_v1.6Q3$ plus $\beta1$ were faster when potentiation was maximal compared to the kinetics during the first depolarization (Fig. 7 *D* and Table 3).

**TABLE 3 Kinetics of activation during repetitive stimulation**

| Channel | $Na_v1.2Q3$ ($n = 6$) | | | $Na_v1.6Q3$ ($n = 4$) | | |
|---|---|---|---|---|---|---|
| Depolarization no. | 1 | 10 | 200 | 1 | 30 | 200 |
| Activation $\tau_{fast}$ (ms) | 0.59 ± 0.11 | 0.54 ± 0.11 | 0.54 ± 0.10 | 0.51 ± 0.14 | 0.44 ± 0.13 | 0.44 ± 0.13 |
| Activation $\tau_{slow}$ (ms) | ND* | ND* | ND* | 4.65 ± 0.83 | 3.33 ± 0.43 | 3.35 ± 0.45 |
| Percentage of $\tau_{fast}$ (%) | ND* | ND* | ND* | 84 ± 5 | 88 ± 2 | 88 ± 2 |

*Not determined because the activation of $Na_v1.2Q3$ was best fit with a single exponential equation.

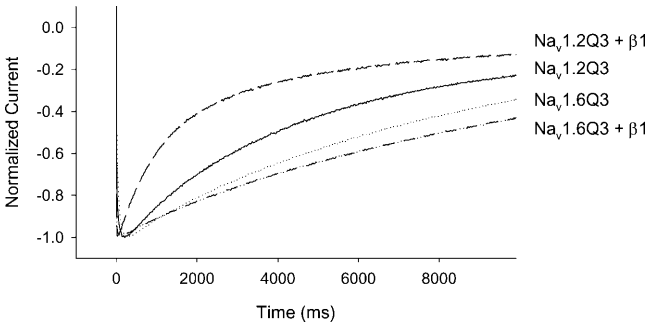


FIGURE 8 Slow-inactivation kinetics of $Na_v1.2Q3$ and $Na_v1.6Q3$ with and without $\beta1$. Oocytes were depolarized from −120 mV to −10 mV for 10 s. The currents were normalized to the peak current amplitude for each depolarization. The data were recorded using the cut-open oocyte voltage clamp as described in Materials and Methods.

Rapid stimulation resulted in both faster activation and faster inactivation of $Na_v1.6$ sodium channels. A single mechanism that could account for acceleration of both activation and inactivation is increased synchronization, because inactivation is coupled to activation in neuronal sodium channels (Aldrich et al., 1983). Sodium channels pass through multiple closed states before opening, which causes a delay in channel opening after depolarization (Armstrong and Gilly, 1979; Keynes and Elinder, 1998; Vandenberg and Bezanilla, 1991). Rapid stimulation might drive the channels into a later closed state and they don't revert to the most extreme closed state between depolarizations, which could result in more synchronous opening and inactivation.

The fact that potentiation occurred with only $Na_v1.6$ and not with $Na_v1.2$ probably reflects differences in both the activation and slow-inactivation kinetics of these two channels. Although both $Na_v1.2Q3$ and $Na_v1.6Q3$ coexpressed with $\beta1$ demonstrated faster activation after repetitive depolarization, the acceleration was more pronounced for $Na_v1.6Q3$. This difference might reflect the fact that activation of $Na_v1.6Q3$ was slower than that of $Na_v1.2Q3$. In addition, only $Na_v1.6Q3$ demonstrated a slow component of activation with $\beta1$, and it was this component that was accelerated most dramatically by rapid stimulation (Table 3). The kinetics of activation for $Na_v1.2$ with $\beta1$ may already be close to the maximal rate, so that repetitive depolarizations did not have much of an effect. In addition to the differences with respect to activation, there was a significant difference between the two channels with respect to slow inactivation. Slow inactivation of $Na_v1.2Q3$ was much faster than that of $Na_v1.6Q3$, and $\beta1$ accelerated the slow inactivation of $Na_v1.2Q3$ while slowing the slow inactivation of $Na_v1.6Q3$. Therefore, the fact that potentiation of current through $Na_v1.2Q3$ with rapid stimulation was transient could be due to channels entering the slow inactivated state. $Na_v1.6Q3$ showed a similar but delayed decrease in current, most likely because slow inactivation in $Na_v1.6Q3$ was less rapid than slow inactivation in $Na_v1.2Q3$. The fact that potentiation continued for 200 depolarizations for $Na_v1.6$ but was transient for $Na_v1.6Q3$ may indicate that fast inactivation affects the kinetics of slow inactivation, either by slowing entry into the slow inactivated state or accelerating recovery from that state.

**TABLE 4 Kinetics of slow inactivation**

| Channel | $Na_v1.2Q3$ | | $Na_v1.6Q3$ | |
|---|---|---|---|---|
| Subunits ($n$) | $\alpha$ (3) | $\alpha + \beta1$ (9) | $\alpha$ (5) | $\alpha + \beta1$ (6) |
| Inactivation $\tau_{fast}$ (ms) | 3.09 ± 0.57 | 1.09 ± 0.14 | 1.93 ± 0.86 | 1.38 ± 0.35 |
| Inactivation $\tau_{slow}$ (ms) | 11.91 ± 1.77 | 7.03 ± 1.72 | 10.08 ± 1.91 | 13.33 ± 2.86 |
| Percentage of $\tau_{fast}$ (%) | 58 ± 3 | 62 ± 7 | 6 ± 3 | 5 ± 1 |

The differences between $Na_v1.6$ and $Na_v1.2$ in their responses to repetitive depolarizations may be important for the physiological roles of the different channels. Nodes of Ranvier develop at sites that contain clusters of sodium channels. The initial clusters contain $Na_v1.2$ and the $\beta2$-subunit (Kaplan et al., 2001), but $Na_v1.2$ is then replaced by $Na_v1.6$ when myelination occurs (Boiko et al., 2001). In the mature neurons, $Na_v1.6$ is localized at nodes of Ranvier whereas $Na_v1.2$ is localized in the unmyelinated regions (Boiko et al., 2001). It may be advantageous to have sodium channels that can faithfully propagate high frequencies of action potentials without loss of amplitude. Slow inactivation could decrease the amplitude or frequency of the spike train and could also result in fewer channels being available for the next wave of stimulation, which might cause a loss of information transmission. The difference in response of the two channels to repetitive depolarizations suggests that $Na_v1.6$ with $\beta1$ would be more able to keep up with multiple rapid stimulations compared to $Na_v1.2$.

Colbert et al. (1997) have shown that sodium current in the soma and dendrites of CA1 pyramidal neurons decreased to ~37 and 73% of their original levels during 10 2-ms depolarizations to −10 mV at 20 Hz. They attributed the current decrease to slow inactivation of the channels. Compared to these results, the potentiation that we observed for $Na_v1.6$ with $\beta1$ during 2-ms depolarizations at 10 Hz was quite small, and the current decrease for $Na_v1.2$ with $\beta1$ was $<1\%$. These differences probably reflect differences in the two sets of experimental conditions. Colbert et al. (1997) recorded from neurons at 37°C. Gating is much faster in those conditions, with full activation and inactivation within 2 ms compared to 20 ms in oocytes at 20°C. In addition, neurons contain multiple sodium channel isoforms including $Na_v1.1$, $Na_v1.2$, and $Na_v1.6$ and associated $\beta$-subunits, whereas we recorded from oocytes expressing a single sodium channel $\alpha$-subunit isoform. Despite the quantitative differences between our results and those obtained from neurons, it is probable that the qualitative differences that we observed between the responses to repetitive depolarizations of $Na_v1.6$ and $Na_v1.2$ sodium channels will be observed in vivo.

However, a true test of the physiological significance of $Na_v1.6$ use-dependent potentiation requires recording from neurons expressing isolated populations of either $Na_v1.6$ or $Na_v1.2$.

We thank Jay Spampanato, Annie Lee, A. J. Barela, and Hai Nguyen for helpful discussions and Brian Tanaka for excellent technical assistance.

This work was supported by the National Institutes of Health (grants NS26729 and NS48336). Wei Zhou was supported by a fellowship from the American Heart Association.

## REFERENCES

Aldrich, R. W., D. P. Corey, and C. F. Stevens. 1983. A reinterpretation of mammalian sodium channel gating based on single channel recording. *Nature*. 306:436–441.

Armstrong, C. M., and W. F. Gilly. 1979. Fast and slow steps in the activation of sodium channels. *J. Gen. Physiol.* 74:691–711.

Boiko, T., M. N. Rasband, S. R. Levinson, J. H. Caldwell, G. Mandel, J. S. Trimmer, and G. Matthews. 2001. Compact myelin dictates the differential targeting of two sodium channel isoforms in the same axon. *Neuron*. 30:91–104.

Caldwell, J. H., K. L. Schaller, R. S. Lasher, E. Peles, and S. R. Levinson. 2000. Sodium channel Nav1.6 is localized at nodes of Ranvier, dendrites, and synapses. *Proc. Natl. Acad. Sci. USA*. 97:5616–5620.

Catterall, W. A. 2000. From ionic currents to molecular mechanisms: the structure and function of voltage-gated sodium channels. *Neuron*. 26:13–25.

Colbert, C. M., J. C. Magee, D. A. Hoffman, and D. Johnston. 1997. Slow recovery from inactivation of Na+ channels underlies the activity-dependent attenuation of dendritic action potentials in hippocampal CA1 pyramidal neurons. *J. Neurosci.* 17:6512–6521.

Goldin, A. L. 1991. Expression of ion channels by injection of mRNA into Xenopus oocytes. *Methods Cell Biol.* 36:487–509.

Goldin, A. L. 2001. Resurgence of sodium channel research. *Annu. Rev. Physiol.* 63:871–894.

Goldin, A. L. 2002. Evolution of voltage-gated Na+ channels. *J. Exp. Biol.* 205:575–584.

Goldin, A. L., R. L. Barchi, J. H. Caldwell, F. Hofmann, J. R. Howe, J. C. Hunter, R. G. Kallen, G. Mandel, M. H. Meisler, Y. Berwald-Netter, M. Noda, M. M. Tamkun, S. G. Waxman, J. N. Wood, and W. A. Catterall. 2000. Nomenclature of voltage-gated sodium channels. *Neuron*. 28:365–368.

Kaplan, M. R., M.-H. Cho, E. M. Ullian, L. L. Isom, S. R. Levinson, and B. A. Barres. 2001. Differential control of clustering of the sodium channels Nav1.2 and Nav1.6 at developing CNS nodes of Ranvier. *Neuron*. 30:105–119.

Keynes, R. D., and F. Elinder. 1998. On the slowly rising phase of the sodium gating current in the squid giant axon. *Proc. R. Soc. Lond. B. Biol. Sci.* 265:255–262.

Litt, M., J. Luty, M. Kwak, L. Allen, R. E. Magenis, and G. Mandel. 1989. Localization of a human brain sodium channel gene (SCN2A) to chromosome 2. *Genomics*. 5:204–208.

Malo, M. S., B. J. Blanchard, J. M. Andresen, K. Srivastava, X.-N. Chen, X. Li, E. W. Jabs, J. R. Korenberg, and V. M. Ingram. 1994. Localization of a putative human brain sodium channel gene (SCN1A) to chromosome band 2q24. *Cytogenet. Cell Genet.* 67:178–186.

Malo, D., E. Schurr, J. Dorfman, V. Canfield, R. Levenson, and P. Gros. 1991. Three brain sodium channel alpha-subunit genes are clustered on the proximal segment of mouse chromosome 2. *Genomics*. 10:666–672.

Novakovic, S. 1999. Sodium channel isoform localization in the peripheral nerve and changes following injury. 1732.

Plummer, N. W., J. Galt, J. M. Jones, D. L. Burgess, L. K. Sprunger, D. C. Kohrman, and M. H. Meisler. 1998. Exon organization, coding sequence, physical mapping, and polymorphic intragenic markers for the human neuronal sodium channel gene SCN8A. *Genomics*. 54:287–296.

Pugsley, M. K., and A. L. Goldin. 1998. Effects of bisaramil, a novel class I antiarrhythmic agent, on heart, skeletal muscle and brain Na channels. *Eur. J. Pharmacol.* 342:93–104.

Smith, R. D., and A. L. Goldin. 1998. Functional analysis of the rat I sodium channel in *Xenopus* oocytes. *J. Neurosci.* 18:811–820.

Smith, M. R., R. D. Smith, N. W. Plummer, M. H. Meisler, and A. L. Goldin. 1998. Functional analysis of the mouse Scn8a sodium channel. *J. Neurosci.* 18:6093–6102.

Spampanato, J., A. Escayg, M. H. Meisler, and A. L. Goldin. 2001. Functional effects of two voltage-gated sodium channel mutations that cause generalized epilepsy with febrile seizures plus type 2. *J. Neurosci.* 21:7481–7490.

Vandenberg, C. A., and F. Bezanilla. 1991. A sodium channel gating model based on single channel, macroscopic ionic, and gating currents in the squid giant axon. *Biophys. J.* 60:1511–1533.

West, J. W., D. E. Patton, T. Scheuer, Y. Wang, A. L. Goldin, and W. A. Catterall. 1992. A cluster of hydrophobic amino acid residues required for fast Na+ channel inactivation. *Proc. Natl. Acad. Sci. USA*. 89: 10910–10914.